Biochimica et Biophysica Acta 1808 (2011) 1728–1736

Contents lists available at ScienceDirect

Biochimica et Biophysica Acta

journal homepage: www.elsevier.com/locate/bbamem

A patch clamp study on the electro-permeabilization of higher plant cells: Supra-physiological voltages induce a high-conductance, K^+ selective state of the plasma membrane

Lars H. Wegner [a,b,*], Bianca Flickinger [a], Christian Eing [a], Thomas Berghöfer [a], Petra Hohenberger [b], Wolfgang Frey [a], Peter Nick [b]

[a] Karlsruhe Institute of Technology, Institute for Pulsed Power and Microwave Technology (IHM), Campus North, 76344 Eggenstein-Leopoldshafen, Germany
[b] Karlsruhe Institute of Technology, Botanical Institute I—Molecular Cell Biology, Campus South, 76131 Karlsruhe, Germany

ARTICLE INFO

Article history:
Received 17 November 2010
Received in revised form 26 January 2011
Accepted 28 January 2011
Available online 4 February 2011

Keywords:
Electroporation
Threshold potential
Patch clamp
Tobacco cell culture
Bright yellow-2 (BY-2)

ABSTRACT

Permeabilization of biological membranes by pulsed electric fields ("electroporation") is frequently used as a tool in biotechnology. However, the electrical properties of cellular membranes at supra-physiological voltages are still a topic of intensive research efforts. Here, the patch clamp technique in the whole cell and the outside out configuration was employed to monitor current–voltage relations of protoplasts derived from the tobacco culture cell line "Bright yellow-2". Cells were exposed to a sequence of voltage pulses including supra-physiological voltages. A transition from a low-conductance (~0.1 nS/pF) to a high-conductance state (~5 nS/pF) was observed when the membrane was either hyperpolarized or depolarized beyond threshold values of around −250 to −300 mV and +200 to +250 mV, respectively. Current–voltage curves obtained with ramp protocols revealed that the electro-permeabilized membrane was 5–10 times more permeable to K^+ than to gluconate. The K^+ channel blocker tetraethylammonium (25 mM) did not affect currents elicited by 10 ms-pulses, suggesting that the electro-permeabilization was not caused by a non-physiological activation of K^+ channels. Supra-physiological voltage pulses even reduced "regular" K^+ channel activity, probably due to an increase of cytosolic Ca^{2+} that is known to inhibit outward-rectifying K^+ channels in Bright yellow-2 cells. Our data are consistent with a reversible formation of aqueous membrane pores at supra-physiological voltages.

1. Introduction

The (transient) permeabilization of the cellular membrane by exposure of cells to a pulsed electric field of high intensity, usually known as "electroporation," is frequently used in biotechnological applications, for instance, in genetic engineering as a tool for introducing DNA into target cells [1]. Electroporation was also successfully employed to optimize the release of cellular ingredients from plant tissues, e.g., sugars from sugarbeet [2], or to decontaminate waste water from bacteria [3,4]. Despite numerous experimental and theoretical studies, many aspects of "electroporation" are still poorly understood, including the physical nature and the molecular properties of the pores generated by membrane charging [1,5–8].

Usually, electroporation is studied by exposing a cell suspension to a homogeneous electric field generated by two external electrodes. Under these conditions, however, membrane charging is highly inhomogeneous. At the poles of a spherical cell, maximum deflections of the native membrane potential occur that are opposite in sign, depending on the orientation towards the cathode and the anode, respectively [9]. By contrast, the membrane potential remains unaffected at the cell equator. To study the electrical properties of cellular membranes at supra-physiological voltages, it would be most adequate to record trans-membrane currents for *homogeneous* charging of the membrane. This can be achieved conveniently by applying the patch clamp technique in the whole cell configuration [10]. However, surprisingly few attempts have been made so far to make use of the patch clamp technique in research on electroporation. O'Neil and Tung [11] used voltage ramps in the cell-attached configuration of the patch clamp technique to determine threshold potentials for membrane breakdown on cardiac tissue. Threshold potentials were highly variable, ranging from 0.6 to 1.1 V. Interpretation of the data was hampered by highly non-stationary conditions during voltage ramp application; moreover, the status of the cellular membrane in series with the patch, and the status of the seal (attachment of the membrane surface to the glass), were not well defined. Tovar and Tung [12,13] repeated these patch clamp experiments

Abbreviations: BSA, bovine serum albumin; BTP, Bis–Tris propane; BY-2, Bright yellow-2; EGTA, ethylene glycol tetraacetic acid; $E_{rev.}$, reversal potential; NTORK, *Nicotiana tabacum* outward rectifying K^+ channel; SD, standard deviation; SE, standard error; TEA, tetraethylammonium

* Corresponding author at: Plant Bioelectrics Group, Karlsruhe Institute of Technology, Campus North, Building 630, Hermann-v-Helmholtz Platz 1, 76344 Eggenstein-Leopoldshafen, Germany. Tel.: +49 721 60824302; fax: +49 721 60822823.
E-mail address: Lars.Wegner@ihm.fzk.de (L.H. Wegner).

0005-2736/$ – see front matter © 2011 Elsevier B.V. All rights reserved.
doi:10.1016/j.bbamem.2011.01.016

using rectangular pulses of 5 or 10 ms duration, but the same critical points with respect to the status of the seal and the cellular membrane apply to those studies. More recently, Pakhomov et al. [14,15] used the patch clamp technique to monitor effects of pulsed electric fields on membrane conductance, but these referred to membrane properties *after* pulse application.

So far, electroporation has been investigated with a medical background and a focus on mammalian cells, and much less work has been dedicated to plant cells, even though practical application of the technique also includes plant cells and tissues. In a series of early studies, Coster et al. [16,17] investigated the effect of supra-physiological voltages on Characeen cells with voltage and/or current clamp technique using intracellular electrodes. They observed a strong increase in membrane conductance to chloride (see also reference 18) when the membrane was hyperpolarized beyond a threshold potential (−300 to −400 mV, depending on the temperature). This phenomenon is known as the "punch-through" effect. Later, Coster and Zimmermann [19,20] found a strong reversible increase in membrane conductance in the giant marine alga *Valonia utricularis* when the membrane voltage exceeded a (temperature-dependent) "breakdown potential" of about +800 mV. So far, only few attempts have been made to study the effect of supra-physiological voltages on protoplasts derived from higher plant cells with the patch clamp technique. Meissner [21], using isolated plant vacuoles in the "vacuole attached" (analogous to the "cell attached") configuration, observed electroporation of the patch enclosed by the pipette tip when the membrane was charged beyond about −300 mV and +250 mV. At these voltages, the rest of the membrane remained intact; further charging led to a complete electroporation of the vacuole.

In this study, we made use of the patch clamp technique to analyze the response of the plasma membrane to homogeneous charging, including supra-physiological voltages. We used protoplasts that were prepared from the tobacco cell line "Bright yellow-2" (BY-2) by enzymatic digestion of the cell wall [9]. We chose this cell line because it is a widely used model system in plant cell biology [22]. Patch clamp experiments were performed in the whole cell and the outside out configurations to avoid limitations associated with working on cell attached patches (see above). Current–voltage curves of the plasma membrane were obtained from 10 ms-rectangular pulses in order to identify the threshold potential for membrane permeabilization. Moreover, the ion selectivity of the electro-permeabilized membrane was studied using fast voltage ramps.

2. Materials and methods

2.1. Cell cultivation and protoplast preparation

As a model system, protoplasts derived from the tobacco cell line "Bright yellow-2" (BY-2) were used. Cell cultivation and protoplast isolation were basically performed as described previously [9]. Briefly, cells were grown at 25 °C in a culture cabinet on 4.3 g/l Murashige–Skoog medium (basal salt mixture) complemented with 100 mg/l inositol, 30 g/l sucrose, 200 mg/l KH_2PO_4, 1 mg/l thiamin, 0.2 mg/l 2,4-dichlorophenoxyacetic acid, and solidified with 0.6% (wt./vol.) Phytagel™ (Sigma-Aldrich, Taufkirchen, Germany). The pH was adjusted to 5.8. Cells were sub-cultivated every 3 weeks.

Cells were harvested for protoplast preparation at the age of 18–20 days and transferred to an enzyme cocktail consisting of (% in wt./vol.) 1 cellulase, 0.1 pectolyase, 2 BSA, and 1 mM $CaCl_2$. Osmolality was adjusted to 480 mosmol/kg using mannitol, as verified with a vapor–pressure osmometer (VAPRO 5520; Wescor, Logan, UT, USA). After 10 h incubation at 28 °C in the dark, the suspension was diluted with washing solution containing 1 mM $CaCl_2$ and 480 mM mannitol and the suspension was centrifuged at 100*g* for 10 min (Heraeus Primo R centrifuge; Heraeus, Hanau, Germany); the sediment was re-suspended in washing solution and washed in the same way a second time. Subsequently, protoplasts were allowed to equilibrate for at least 3 h in the bath medium used for patch clamp experiments (see below) to which 10 mM glucose and 10 mM sucrose had been added. In some cases, protoplasts were additionally purified using a sucrose gradient as described by Flickinger et al. [9] before they were transferred to the bath medium.

2.2. Patch clamp procedure

For patch clamp experiments, a standard setup was used including an EPC-10 amplifier (HEKA, Lambrecht, Germany) and an inverted microscope (Axiovert 200 M; Zeiss, Oberkochen, Germany). Micropipettes fabricated from borosilicate glass capillaries (Kimble No. 34500 99; Gerresheimer, Rockwood, TN, USA) were pulled with a 2-step-procedure on a Narishige puller (PE21; Narishige, Tokyo, Japan) and filled with a solution containing (concentrations in mM) 120 K-gluconate, 10 EGTA, 2.68 $MgCl_2$, 3.91 $CaCl_2$, 2.13 Mg-ATP, 2 Mes, with free Ca^{2+} and Mg^{2+} concentrations being 0.1 μM and 2 mM, respectively, as calculated with the computer program "Calcium" [23]. Mannitol was added to a final osmolality of 472 mosmol kg^{-1}. The pH was adjusted to 7.2 with Bis–Tris–Propane (BTP). The bath medium was composed as follows (concentrations in mM): 30 K-gluconate, 5 $CaCl_2$, 2 $MgCl_2$, 10 Mes/BTP, pH 5.8. Although the composition of the solutions did not directly mimic physiological conditions, relevance of patch clamp data for the electroporation of intact cells was ensured by adjusting parameters like ion strength, pH, and free intracellular Ca^{2+} concentration adequately. Standard patch clamp procedures in the whole cell and outside out configuration were applied [10]. Data were recorded with a personal computer (Maxdata) using the PatchMaster v2 ×32 software (HEKA). To explore the electrical membrane properties at supra-physiological voltages, rectangular pulses of 10 ms length were administered with negative and positive voltages at an alternating sequence. Starting at the maximum of −1000/+1000 mV, the amplitude was successively decreased in 40 mV-steps. Alternatively, voltage ramp protocols were used, recording the current response of the plasma membrane. Low-pass filtering of the data at a cutoff frequency of 7.2 MHz was performed; the sampling frequency was adjusted to 66 MHz. In addition, K^+ channel activity was screened with 1.5 s-rectangular pulses ranging from −80 to +160 mV (2.7/10 MHz cutoff/sampling frequency). Liquid junction potentials were corrected for using the procedure of Neher [24].

2.3. Processing of patch clamp data

No attempt was made in whole cell experiments to compensate for cellular capacitance or series resistance (R_s) during data acquisition when 10 ms-pulses were applied. Instead of making use of the "R_s compensation" function of the "PatchMaster" software, the effective voltage drop across the cellular membrane ($V_M(t)$) was estimated *ex post* from the change in command voltage (ΔV_{comm}), the amplitude of the capacitive spike induced by the rectangular voltage drop (I_0), and the current amplitude at the end of the pulse ($I(t)$) according to

$$V_M(t) = V_{comm} - (I(t) / I_0) * \Delta V_{comm} \quad (1)$$

I_o was extrapolated by fitting the capacitive current relaxation with an exponential function:

$$I_{cap}(t) = I_0 * \exp(-t / \tau) \quad (2)$$

A voltage step of several hundred millivolts usually induced a sudden drop in membrane resistance (see below). In the majority of the experiments, the membrane resistance (R_M) roughly equalled the access resistance (R_S) under these conditions; as a consequence, R_M and R_S that are connected in series acted as a voltage divider, and only ~50% of the command voltage dropped across the cellular membrane.

In some experiments, R_S exceeded R_M, (i.e., the command voltage predominantly dropped at R_S instead of R_M); in these cases, the determination of V_M was considered to be too error-prone, and the data were discarded. Current–voltage relations were extracted from current deflections elicited by a series of voltage pulses by plotting current amplitudes measured after 10 ms pulse duration against the corresponding trans-membrane voltage difference with the help of the software package "Origin" (OriginLab Corporation, Northampton, MA, USA).

At supra-physiological voltages, large inward and outward currents were elicited. These currents deactivated rapidly when the voltage was returned to less extreme values. However, the permeabilized state of the membrane persisted when the voltage was rapidly shifted into the physiological range by imposing rapid voltage ramps. From the reversal potential ($E_{rev.}$; the voltage at which net ion transport is zero) of current–voltage relations obtained in this way, further information on the ion selectivity of the membrane at the permeabilized state could be deduced. To this end, the membrane was conditioned by a 10 ms-prepulse to establish the low-conductance or the high-conductance state, respectively. Subsequently, the command voltage was shifted into the positive range at a constant rate of 40 mV/ms. The current response I_{ramp} consisted of a capacitive (I_{cap}) and a resistive (I_{res}) fraction:

$$I_{ramp} = I_{cap} + I_{res} \tag{3}$$

For thermodynamic calculations (see below), the voltage at which $I_{res.} = 0$ was of interest. To this end, I_{ramp} had to be corrected for the capacitive component. For a ramp with a time-invariant slope, I_{cap} renders a constant offset calculated according to [25]:

$$I_{cap} = C_M * dV_M / dt \tag{4}$$

with C_M being the cellular capacitance. Hence,

$$I_{res} = I_{ramp} - C_M * dV_M / dt \tag{5}$$

From the reversal potential, $E_{rev.}$, at $I_{res} = 0$, relative permeabilities of the membrane for K^+ *versus* gluconate can be estimated by using the Goldman equation [26]:

$$E_{rev.} = 59mV * log \frac{P_{K+} / P_{gluconate} [K^+]_o + [gluconate]_i}{P_{K+} / P_{gluconate} [K^+]_i + [gluconate]_o} \tag{6}$$

with $P_{K+}/P_{gluconate}$ being the relative permeability of the membrane for K^+ over gluconate. Indices "o" and "i" stand for "outside" and "intracellular," respectively. Note that this approach ignores putative membrane permeability to other ions (Ca^{2+}, chloride).

3. Results

3.1. Current–voltage relations obtained from whole cell recordings

After establishing the whole cell configuration, the current response of a BY-2 protoplast to 10 ms-rectangular pulses of various magnitudes was recorded in order to elucidate electrical properties of the membrane at supra-physiological voltages. In Fig. 1A, a selection of 4 voltage pulses and the corresponding current traces is depicted for a typical experiment. Stepping the membrane to positive or negative voltages elicited a capacitive current spike that relaxed with a single-exponential time course as described by Eq. 2. At a moderate membrane polarization (e.g., at ±200 mV), the current level almost returned to the value measured before pulse application after about 2 ms. It should be noted that the trans-membrane voltage drop amounted to more than 90% of the applied command voltage at the end of the pulse. When the holding potential was re-established, a second capacitive spike of identical magnitude occurred but with opposite polarity. A more drastic polarization, e.g., at a command voltage of ±720 mV, however, induced a biphasic current response: After a (partial) decay of the capacitive spike, the current passed through a minimum but increased again at a time scale of several ms and tended to saturate at the end of a 10 ms-pulse in the majority of the experiments. The original current level was restored within 2 ms after the membrane was returned to the holding potential; for technical reasons, the time course of recovery could not be analyzed in more detail. In this case, the trans-membrane voltage drop only amounted to about 50% of the command voltage at the end of the pulse; the remaining part dropped at the series resistance, R_S, connecting pipette lumen and cell interior (see Materials and methods).

From the total number of 51 rectangular pulses, a current–voltage curve was inferred for this protoplast as shown in Fig. 1B. The current

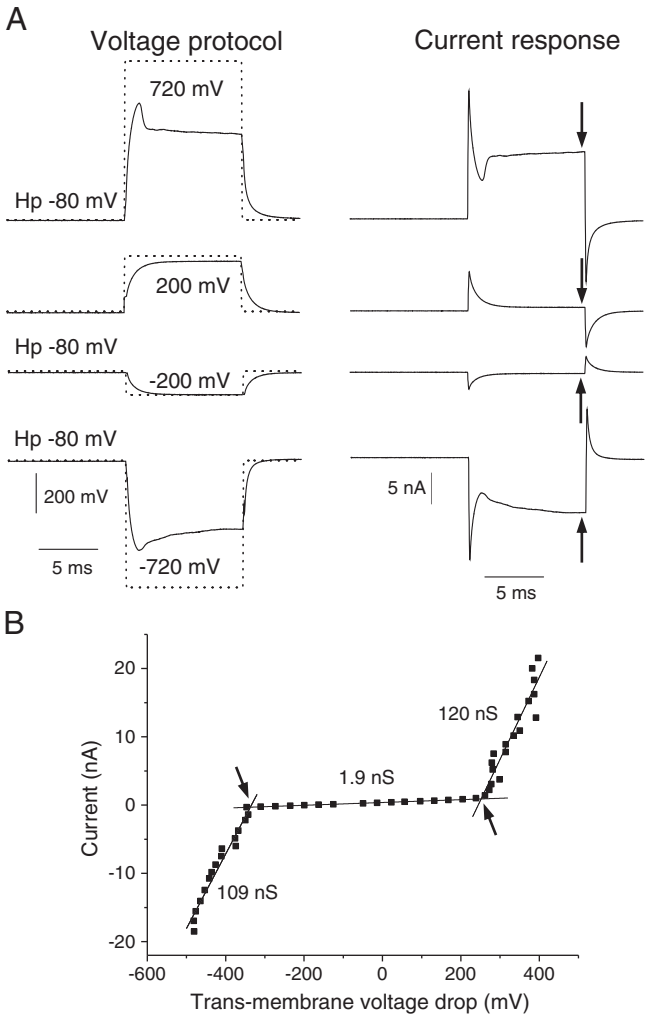

Fig. 1. Challenge of a protoplast clamped in the whole cell configuration by rectangular pulses of 10 ms length covering a broad voltage range. Representative traces of the command voltage (left column, dotted line), the effective trans-membrane potential difference calculated according to Eq. 1 (left column, solid line) and the current response of the cell (right column) are depicted in A for four different pulses. Intermittently, the membrane was clamped to −80 mV throughout the experiment. Note that after 10 ms pulse duration, the trans-membrane voltage drop was only 49% and 59% of the command voltage of +720 and −720 mV, respectively, applied via the patch clamp amplifier. By plotting the current amplitude at the end of the pulse (arrows in A) against the respective trans-membrane voltage difference for $n = 51$ pulses, a current–voltage relation extending far beyond the physiological voltage range was obtained (B). Three segments of the curve could clearly be identified. A low-conductance range extended between the threshold potentials of -337 and +251 mV (arrows in B). Beyond these voltages, membrane conductance increased dramatically. For each segment, the IV-curve was well represented by a linear fit. The conductances calculated from the slopes of the linear fits (solid lines) are given in the figure.

Table 1
Evaluation of current–voltage plots obtained from trains of 10 ms rectangular voltage pulses (compare Figs. 1 and 2; mean values ± standard error).

		Hyper-	De-polarization	Intermediate voltage range
Membrane conductance (G)	Whole cell (nS/pF), $n=9$	5.2 ± 1.1	5.6 ± 1.3	0.10 ± 0.03
	Outside out (nS), $n=3$	12.9 ± 1.7	18.8 ± 3.1	1.8 ± 0.7
Threshold potential	Whole cell (mV), $n=9$	−273 ± 16	205 ± 14	
	Outside out (mV), $n=3$	−292 ± 29	291 ± 27	

amplitude measured after a pulse duration of 10 ms was plotted against the effective trans-membrane voltage difference. At intermediate voltages ranging between about −300 and +250 mV, the IV-curve was flat; from the slope, a conductance of 1.9 nS was calculated by linear regression. Beyond this voltage range, however, the slope increased strongly, leading to a characteristic appearance of the current–voltage relation that is reminiscent of a varistor. Linear fits rendered conductances of 109 nS and 120 nS for the extreme negative and positive voltage range, respectively. Transition between the low and the high conductance state of the membrane occurred in a narrow voltage window that could not be quantified from our measurements; instead, a threshold potential was defined as the voltage at which the linear curve fits intersect. For the experiment shown in Fig. 1B, threshold potentials of −337 mV and +251 mV were determined (arrows in Fig. 1B).

This pattern was confirmed in a set of 8 further whole cell experiments, summarized in Table 1. Conductances were normalized to the cellular capacitance in order to eliminate effects of cell size. The experiments summarized here were performed at different holding potentials; between pulses, the membrane potential was either kept at moderately negative voltages (−90 or −80 mV) corresponding to a conductance minimum known to support membrane stability [27], or it was clamped close to 0 (−10 or 0) mV. No significant difference in conductances or threshold potentials was observed for these various holding potentials (not shown); therefore, data were pooled. Although the threshold voltages varied somewhat among individual experiments (compare, e.g., Fig. 1 with Fig. 5 below), they were always of the same magnitude. There appeared to be a slight asymmetry in the IV curves since the absolute value of the threshold potentials was slightly (but significantly at $P=0.01$; Student's t-test) lower for membrane depolarization as compared to membrane hyperpolarization.

3.2. Current–voltage relations obtained from outside out recordings

Although a rather clear picture emerged from these whole cell experiments, it has to be kept in mind that some simplifying assumptions had to be made in order to arrive at these results (see Materials and methods), especially with respect to the calculation of the effective trans-membrane voltage drop. In order to circumvent this problem, we repeated the experiment on excised patches in the outside out configuration. In this configuration, the voltage difference imposed on the membrane was identical to the command voltage. Original traces obtained from one representative experiment are shown in Fig. 2A, and the corresponding current–voltage relation is depicted in Fig. 2B. When the membrane was stepped from 0 mV to ±160 mV, this was associated with a small shift in the steady current level. A more pronounced polarization in both directions elicited additional components of inward and outward currents that partly activated with a delay of a few milliseconds, in agreement with the whole cell recordings presented above. The same pulse sequence covering the voltage range between −400 and +400 mV was imposed several times and rendered

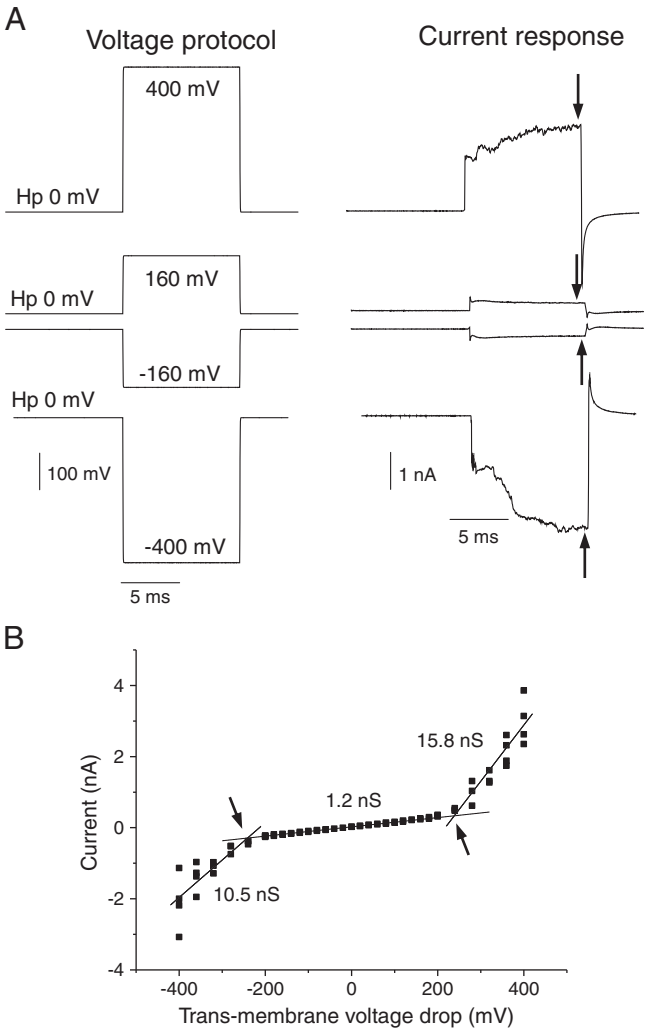

Fig. 2. Current–voltage relation of an outside out patch exposed to rectangular pulses of various magnitudes. Rectangular pulses of different magnitudes (left column) were applied to an outside out patch, and the current response (right column) was recorded; again, four representative pulses were selected for presentation in A. Note that the command voltage was identical to the trans-membrane voltage difference here since no voltage drop at the access resistance had to be taken into account, in contrast to measurements performed in the whole cell configuration (compare Fig. 1A). A plot of the current amplitude after 10 ms pulse duration (arrows in A) against the pulse potential is shown in B. Different current amplitudes recorded at the same voltage result from repetitive application of the same pulse sequence extending from −400 to +400 mV. As shown above for whole cell recordings, three segments of the curve could clearly be discerned: a low-conductance segment ranging between −240 and +239 mV (arrows in B) and two high-conductance segments at the extremes. Linear fits to each segment are indicated by solid lines, and conductances calculated from the slopes are given in the figure.

somewhat different current responses, especially when the membrane was hyperpolarized. This is evident from the current–voltage curve plotted in Fig. 2B. In analogy to the whole cell recordings, conductance was low in the intermediate voltage range around 0 mV and increased strongly when thresholds of –240 and +239 mV, respectively, were exceeded. However, the conductances measured at these extreme values were reduced by more than 10-fold when compared to those found for the whole cell experiments. This was to be expected if those whole cell currents had actually been trans-membrane currents. In case they had mainly originated at the membrane-glass interface (i.e., from a dramatic drop in the seal resistance with extreme voltages due to a (reversible) damage of the seal), the current–voltage profile should have been largely the same in both patch clamp configurations (for a more detailed comparison of whole cell and outside out currents, see the Discussion).

3.3. Selectivity of the cellular membrane at supra-physiological voltages

It was of particular interest to identify the ions that carried large inward and outward currents beyond the threshold potentials. To this end, ramp protocols were additionally imposed as described in Materials and methods. The membrane was polarized for 10 ms to a constant voltage either below or beyond the threshold potential, both in the negative and positive voltage range; subsequently, the polarity was inverted by changing the voltage continuously with time (Fig. 3A; compare Materials and methods for more details on the design of the protocol and data evaluation). As a result, current–voltage plots for the low- and the high-conductance states were obtained successively in whole cell recordings on the same protoplast as exemplified in Fig. 3B (showing the relevant detail of the entire voltage range covered by the ramps). It is obvious that the curves differed in slope by a factor of about 17 (1.9 nS *versus* 32 nS for the ramps started at prepulse potentials of −100 and about −320 mV, respectively), indicating that the high-conductance state was, at least partly, retained during the ramp (even though voltage had entered the "intermediate" range). The current difference between the curves was obviously associated with a preceding membrane permeabilization by extremely negative voltages. Hence, the reversal potential of this additional permeability component was associated with the point at which the two IV-curves intersected, in this case at -26 mV (Fig. 3B; arrow). A similar value for the reversal potential was obtained in 10 other whole cell experiments (mean value ± SD, −27.7 ± 6.8 mV; $n = 11$). In two experiments not included in the statistics, deviating results were obtained ($E_{rev.} = 6$ mV and −4 mV, respectively) for unknown reasons. When this experiment was repeated using *positive* prepulse potentials and subsequent voltage ramps with a negative slope, similar results were obtained for the reversal potential after processing the data as described in Materials and methods; IV curves intersected at −22.4 ± 6.4 mV (mean value ± SD, $n = 5$). Intersection potentials obtained following membrane depolarization and hyperpolarization were not significantly different at $P = 0.05$ (Student's *t*-test).

From the reversal potentials, relative permeabilities of the major ions, K^+ and gluconate could be estimated using the Goldman equation (Eq. 6). For the relative permeability $P_{K+}/P_{gluconate}$, values of 5.3 and 10 were calculated from reversal potentials of -22.4 and −27.7 mV, respectively, indicating that K^+ was transported 5–10 times more readily across the membrane than gluconate. This definitely reflected membrane properties; electrodiffusion constants in solution would result in a $P_{K+}/P_{gluconate}$ ratio of only 1.9 (corresponding to an $E_{rev.}$ value of −10 mV). Additional experiments performed in the outside out configuration confirmed this result. From the experiment shown in Fig. 4, a reversal potential of −25 mV was obtained. For the relative permeability $P_{K+}/P_{gluconate}$, a value of 7.1 was calculated. On average, the reversal potential was determined to be −29 ± 13 mV from outside out

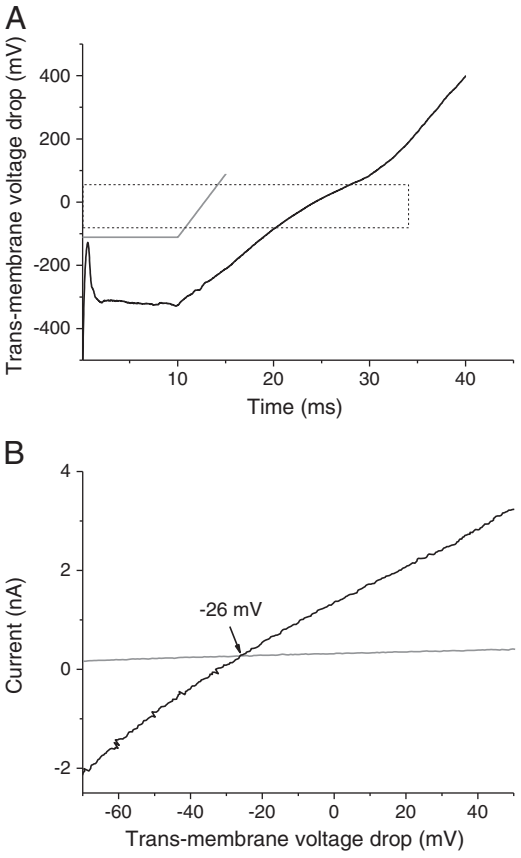

Fig. 3. Current–voltage relations obtained by applying rapid voltage ramps to a protoplast in the whole cell configuration. B shows two current traces as a function of the trans-membrane voltage drop obtained by challenging the same protoplast by two different types of voltage protocols as depicted in A. The gray traces result from a clamp of the cellular membrane potential to −110 mV (intermediate voltage range) for 10 ms; subsequently, the voltage was continuously increased to +90 mV at a rate of 40 mV/ms. The bold trace was obtained by a membrane polarization to about −320 mV for 10 ms (induction of the permeabilized state), followed by a voltage ramp at a rate of about 24 mV/ms. This ramp was shaped by the voltage divider effect occurring in whole cell experiments (see Materials and methods). The voltage range depicted in B corresponds to the dotted box in A. Current traces shown in B were corrected for the capacitive shift as described in Materials and methods. The voltage at which both curves intersect is given in the plot. It represents the reversal potential of the conductance elicited by supra-physiological voltages.

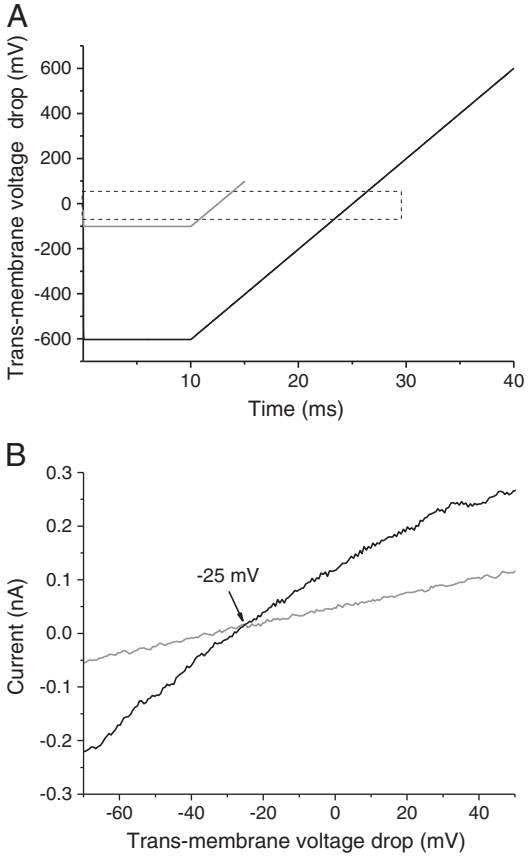

Fig. 4. Current–voltage relations obtained by applying rapid voltage ramps to a patch in the outside out configuration. The same combination of dual voltage protocols (A) was applied as in whole cell experiments (see legend to Fig. 3 for details) but without any voltage divider effect. Therefore, prepulse potentials were −100 and −600 mV (gray and bold trace, respectively), and the voltage was subsequently changed at the same rate (40 mV/ms). As in Fig. 3, the dotted box indicates the voltage range chosen for presentation in B. Note that current–voltage curves intersected at −25 mV, very close to the voltage determined in the whole cell experiment.

Table 2
Summary of Boltzmann parameters (Eq. 7) for the K^+ outward rectifier before ("prepulse") and after ("postpulse") administration of 5 supra-physiological 10 ms-voltage pulses ($n=3$).

	Prepulse	Postpulse
Maximum K^+ conductance (rel. units)	1^{aa}	0.36 ± 0.12^{bb}
Apparent minimum gating charge, δ	2.91 ± 0.43	2.58 ± 0.90
Midpoint potential (mV), $V_{1/2}$	14.4 ± 13.6^{a}	54.1 ± 20.8^{b}

Mean values ± SD are given. ^{aa,bb} = significantly different at $P=0.05$. ^{a,b} = significant at $P=0.1$ (Student's *t*-test).

experiments (mean value ± SD, $n=5$; negative prepulse); this corresponded to a mean $P_{K+}/P_{gluconate}$ value of 12.5.

3.4. Effects of supra-physiological voltages on K^+ channel activity

A preference for K^+ *versus* the anion gluconate might indicate that the conductance increase at extreme voltages was, at least in part, due to the activation of K^+ channels. Both inward- and outward-rectifying K^+ channels have been characterized during electrophysiological studies on BY-2 protoplasts [27–30; see also data below] and after cloning of K^+ channel genes from BY-2 cells and heterologous expression in oocytes [30]. Voltage dependence of these K^+ channels that are active in the physiological voltage range deviates strongly from that reported here (see also below, Table 2); however, it was proposed previously that ion channels may be "damaged" by supra-physiological voltages and may thus exhibit an additional "artificial" voltage dependence [31,32] in response to an extreme polarization of the membrane. In order to test this hypothesis, current–voltage relations in the whole cell configuration covering the supra-physiological voltage range were recorded before and after administration of the K^+ channel blocker tetraethylammonium (TEA^+) at a concentration of 25 mM that is known to inhibit inward and outward rectifying K^+ channels in BY-2 cells [29]. As shown in Fig. 5, addition of TEA^+ had no effect on the shape of the current–voltage relation; qualitatively similar results were obtained in 3 other independent experiments. This finding is clearly at variance with the model of Tsong [31], at least with respect to electro-permeabilization in BY-2 cells.

However, the blocker study with TEA^+ was not sufficient to refute the hypothesis of Tsong unequivocally since channel properties may be affected in such a way that the inhibitor is no longer effective. Further evidence for a "damage" of K^+ channels may be obtained by monitoring activity of the K^+ outward rectifier prior to and after challenging the protoplast with supra-physiological voltages. To this end, 1.5 s rectangular pulses were applied in the physiological voltage range before treatment and immediately after imposing 5 pulses to supra-physiological (positive) voltages. Results are summarized in Fig. 6. Current traces elicited by challenging a protoplast with this protocol are depicted in Fig. 6A. It is obvious from these data that delayed outward currents carried by K^+ channels (NTORK1; [30]) were *reduced* by an extreme polarization of the membrane. This was also reflected by the current–voltage curves shown in Fig. 6B that were calculated from the original traces as exemplified in Fig. 6A; currents were reduced by more than 60% in this experiment. After establishing the whole cell configuration, K^+ channel activity was repetitively screened in order to make sure that it was constant and invariant with time; this is shown by plotting the current amplitude *versus* time (together with the voltage protocol) in Fig. 6C. Successively, 5 pulses to about 250 mV were applied at an interval of about 10 s, and a sustained reduction of K^+ channel activity was monitored using the same pulse sequence as before. Changes in gating properties of K^+ channels induced by supra-physiological voltages were analyzed by applying a Boltzmann formalism as described previously [32–34]. Briefly, the amplitude of tail currents recorded after repolarization of the membrane at the end of each pulse was measured; current amplitudes were leak-corrected, normalized, and plotted against the voltage applied during the preceding conditioning pulse (Fig. 6D). Fitting the data with a Boltzmann equation (see caption of Fig. 6) revealed a positive shift of the midpoint potential (i.e., the voltage at which 50% of the whole channel population was in the open state) by a treatment of the membrane with strong electric fields (Table 2). The apparent minimum gating charge was not affected significantly. These data confirmed that treatment with supra-physiological voltages had an effect on gating of K^+ channels, but channel activity was *reduced* instead of being enhanced. Activity of the K^+ inward rectifier that was only sporadically observed in whole cell experiments was also not enhanced by supra-physiological voltage pulses (data not shown).

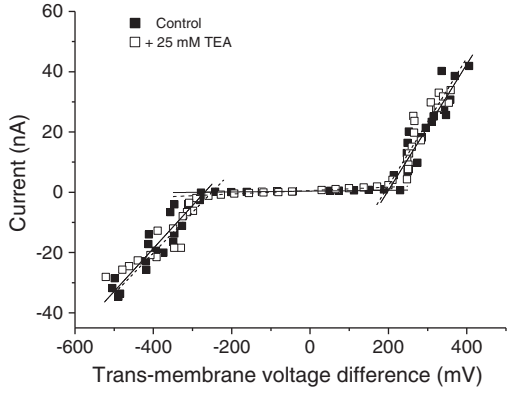

Fig. 5. Effect of TEA^+ on the current–voltage curves of BY-2 protoplasts. Almost identical current–voltage curves were obtained on a protoplast challenged with 10 ms voltage pulses before and after the addition of 25 mM TEA-nitrate to the bath (whole cell configuration; compare Fig. 1). Three segments of the IV could again be identified and linear fits were applied separately (solid lines, control; dotted lines, $+TEA^+$). Slope values were (control/TEA^+, in nS): 143/135 (hyperpolarization); 1.3/5 (intermediate range); 209/211 (depolarization). Threshold potentials were −268/−258 mV (hyperpolarization); 200/198 mV (depolarization).

4. Discussion

4.1. Studying electroporation with the patch clamp technique on protoplasts derived from tobacco culture cells: comparison with other techniques and cell types

Polarization of the membrane beyond a certain threshold potential induced a dramatic increase in membrane conductance in patch clamp experiments on BY-2 protoplasts both in the whole cell and the outside out configuration. At first glance, this response is reminiscent of the "punch through" effect described for strongly hyperpolarized Characeen cells [16,17]. However, in *Chara*, large Cl^- currents are activated at a time scale of seconds, whereas in BY-2 cells, both inward and outward currents (predominantly carried by K^+) are elicited in the millisecond and sub-millisecond range once the voltage exceeds the threshold potential. The effects described in this communication are more similar to dielectric breakdown reported for the marine alga *V. utricularis* that is obviously brought about by a mechanism very different from the "punch through" effect in *Chara* [19]. However, *V. utricularis* is not a good model system for (higher) plant cells because of the physiological and structural peculiarities of this species [35,36]. Moreover, current–voltage curves recorded on these cells result from two membranes in series, plasma membrane and tonoplast, since intracellular microelectrodes are always inserted into the vacuole that takes more than 95% of the cell volume. The data obtained on protoplasts derived from BY-2 cells are more representative of plant cells (and eukaryotic cells in general) and, hence, are more apt to improve our basic understanding of the dielectric breakdown of the plasma membrane.

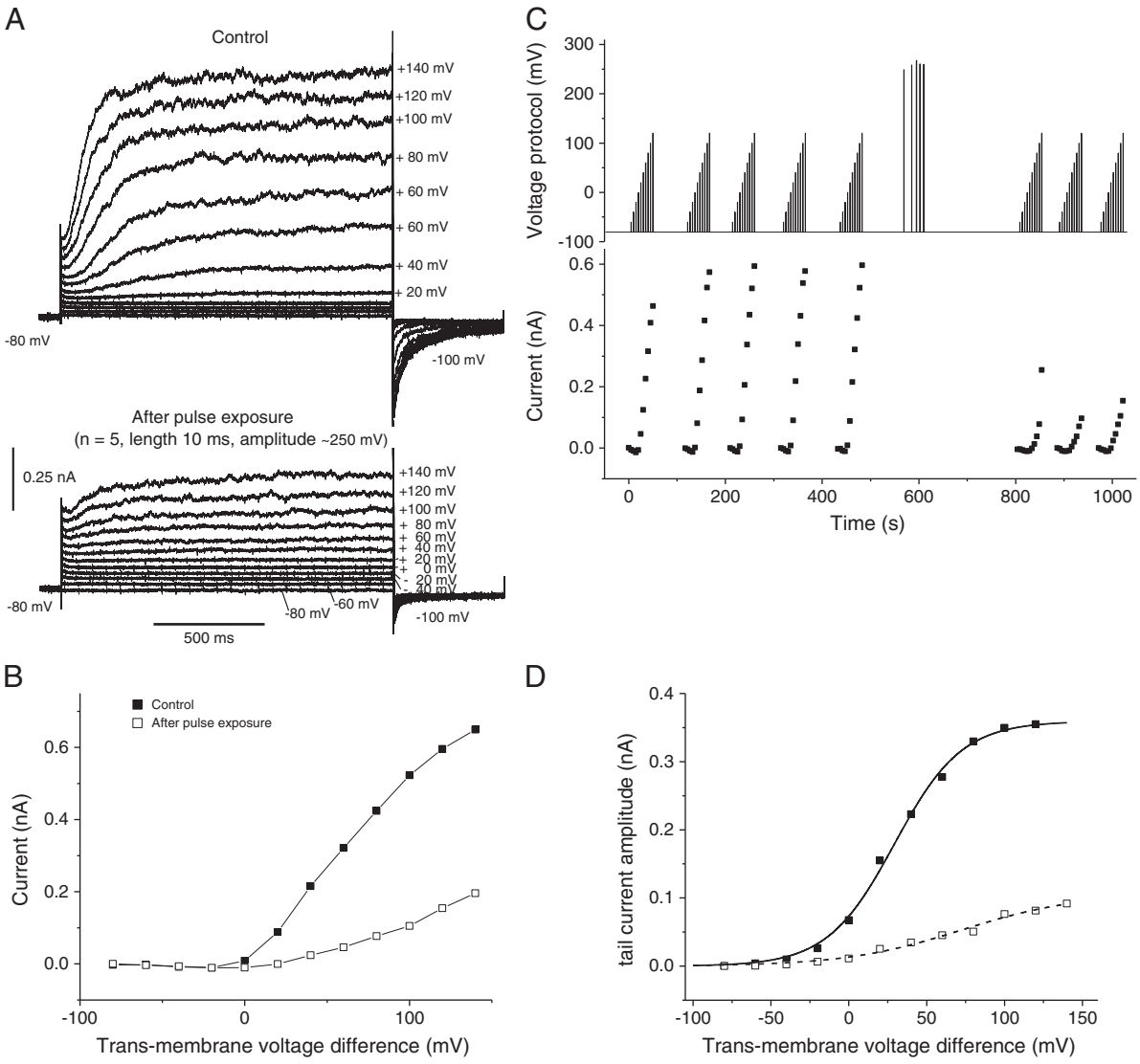

Fig. 6. Whole cell K^+ currents elicited by a prolonged membrane depolarization in a protoplast under control conditions and after stepping the membrane potential 5 times to about 250 mV for 10 ms. In A, current traces elicited by moderate, positive-going voltage pulses of increasing amplitude are superimposed; the pulse potential is given at each trace. Following a rectangular pulse of 1.5 s length, the membrane was repolarized to −100 mV for 1 s. Between individual pulses, the membrane was clamped to a holding potential of −80 mV for 5 s. It is obvious that the amplitude of slowly activating currents decreased after challenging the membrane with extreme voltages. B, current–voltage plots obtained from the data shown in A (see legend in the figure); steady state currents after subtraction of the instantaneous "leak" component are plotted. C, protocol of the experiment with time (upper panel, clamped voltage; lower panel, current response). Under control conditions, the same voltage protocol was applied 5 times in order to make sure that K^+ channel activity was stable with time. Subsequently, 10 ms-pulses were applied, and K^+ channel activity was monitored again three times. Currents were strongly reduced by the pulses. D, tail current amplitudes (I_{tail}) measured at −100 mV plotted as a function of the voltage applied during the preceding 1.5 s-depolarizing pulse (V). To characterize gating properties, data were fitted with a Boltzmann equation: $I_{tail} = \frac{I_{tail,max}}{1 + \exp\{(V_{1/2} - V) * \delta * F / RT\}}$ (Eq. 7), with $I_{tail,\,max}$ = maximum current amplitude, $V_{1/2}$ = midpoint potential, δ = apparent minimum gating charge. *R*, *F*, and *T* have their usual meaning. Parameters obtained from the fit were (control/after pulsing) $I_{tail,\,max}$ = 0.36/0.11 nA; $V_{1/2}$ = 29.4/72.4 mV; δ = 2.7/1.6.

Recently, Flickinger et al. [9] used BY-2 protoplasts stained with the voltage-sensitive dye ANNINE-6 to monitor the generation of a trans-membrane potential difference by exposure to an external electrical field. It was concluded from these measurements that membrane permeabilization started at a membrane potential difference of about 300 mV. Patch clamping performed in this study rendered similar or slightly lower values, even though the pulse duration was very different in both studies (1 μs *versus* 10 ms); note that pulses in the sub-millisecond range cannot be applied in a controlled way via the patch pipette for technical reasons. Despite this limitation of temporal resolution, studying electroporation with the patch clamp technique has several advantages over alternative techniques: (i) the membrane is homogeneously charged to a defined value; and (ii) most importantly, currents passing the membrane at supra-physiological voltages can directly be measured. This opens up the possibility of a more detailed characterization of the membrane in the permeabilized state, e.g., with respect to relative permeabilities for the ions that permeate the membrane at this conductance state (Figs. 4 and 5). Hence, the patch clamp technique is a useful tool in electroporation research that has hitherto clearly been undervalued (see Introduction).

Although plant cell protoplasts are a useful and convenient system for studying electroporation in a defined way, it has to be pointed out that they are not representative of an intact plant cell in all respects. Therefore, extrapolation of the results to a true *in vivo* situation has to be done with care.

4.2. Outside out versus whole cell recordings

When outside out patches were exposed to a sequence of 10 ms-pulses, results were qualitatively similar to those obtained in the whole cell configuration (compare Figs. 1 and 2). However, the threshold

potential was significantly higher for membrane depolarization in outside-out patches. Conductances at extreme voltages differed by a factor of only about 10. This is much less than expected from the difference in the exposed membrane surface in both configurations [10]. However, a comparison of the data obtained in both configurations is not straightforward. Outside-out data are not compromised by the discrepancy between clamped potential and actual trans-membrane voltage drop [25], and capacitive effects interfering with the measurements are much reduced with respect to whole cell recordings, suggesting that excised patches are more suitable for studying electric field effects on membranes. However, it has to be kept in mind that, in excised patches, the membrane is in an unnaturally bent state; this mechanical stress (that is absent in the whole cell configuration) may also affect the results; mechanical deformation of the membrane aspired into the patch pipette was previously considered to be the main reason why Ca^{2+} channel activity in single patches did not match the values calculated from whole cell recordings (e.g., reference 37).

4.3. Currents elicited at supra-physiological voltages are most likely not carried by K^+ channels

The observation that the membrane in the electro-permeabilized state bore some selectivity for K^+ over the organic anion gluconate (Figs. 3 and 4) prompted us to test the hypothesis that K^+ channels may at least contribute considerably to the currents recorded at supra-physiological potentials. Both inward and outward rectifying K^+ channels co-exist in the plasma membrane of BY-2 cells. However, these channels are activated in the physiologically relevant voltage range and attain maximum open probability at potentials near the threshold for transition between low and high conductances determined in this study ([27,29]; Fig. 6, this study), which has been confirmed by heterologous expression of these channels in oocytes [30]. Moreover, the data that are available on these K^+ channels, e.g., on the outward rectifier NTORK, suggest that they could not give rise to the extremely large current densities reported here (Table 1). However, some authors [31] hypothesized that (voltage-sensitive) ion channels may sense the extremely strong local field in the membrane that is generated by supra-physiological membrane potentials, and may be "dragged open" under these conditions. In order to test for this possibility, we applied the K^+ channel blocker TEA^+ that is known to block K^+ channel activity in BY-2 cells [29], but no effect on the supra-physiological current–voltage curve of protoplasts was observed (Fig. 5). This provides evidence against a major contribution of K^+ channels to the voltage-induced permeability increase. It could be argued, though, that the channel structure (with several subunits forming a pore; [38]) is affected by the electrical field in such a way that the blocker is no longer effective.

Unfortunately, it is not possible with our experimental approach to quantify ion channel activity during the application of supra-physiological voltage pulses; however, some information on the effect of high voltages on channel activity can be inferred from a comparison of K^+ channel activity recorded before and after the application of a series of 10 ms-pulses to voltages exceeding the threshold potential (Fig. 6, Table 2). It was found that pre-treatment by extreme voltages even reduced the activity of the dominant outward-rectifying K^+ channels in BY-2 cells by at least 50%, suggesting that these channels do not play a major role in membrane permeabilization by electrical fields. The inhibitory effect of supra-physiological voltage pulses on the K^+ outward rectifier reported here can be explained by its sensitivity to cytosolic Ca^{2+}. Electroporation favors an increase in the cytosolic Ca^{2+} concentration in BY-2 cells [39]. It has been demonstrated previously that the K^+ outward rectifier in BY-2 protoplast [29] and other plant cells [40] is down-regulated by elevated cytosolic Ca^{2+} concentrations. EGTA was included in the pipette medium to keep the cytoplasmic Ca^{2+} concentration at the desired value (0.1 μM). However, experiments on guard cell protoplasts [41] have shown that EGTA included in the pipette solution does not prevent a massive Ca^{2+} influx into the cytoplasm as expected to occur during electro-permeabilization of the membrane. On the basis of our data, it cannot completely be ruled out that the K^+ outward rectifier (or some other K^+ selective channel or transporter) is modified by extreme voltages generating a high conductance state. No experimental evidence for the activation of ion channels by supra-physiological membrane potentials was obtained in this study, but the possibility remains that transporters damaged by a strong electrical field lost activity upon return to physiological clamp voltages.

A reduction in K^+ channel activity in response to pulsed electric fields was also reported for skeletal muscle fiber cells [32,42,43]. The authors suggested that this effect on ion channel activity resulted from a direct field effect on the protein structure. Independent of different mechanistic interpretations, the effects observed on BY-2 cells and on skeletal muscle fibers bore some similarities but are at variance with the predictions of a non-physiological "burst" of channel activity [27].

4.4. Implications for electroporation theory

Instead, our data are in agreement with the formation of aqueous pores in the membrane as implied by the term "electroporation" and currently favored by the majority of the researchers in this field [1,5–7,44,45]. This does not rule out that intrinsic membrane proteins are involved in the formation of these pores, but the roles of proteins and lipids organized in lipid rafts [46] for "voltage sensing" and pore formation cannot be inferred from our data. A marked selectivity for K^+ over gluconate may be explained by the small size of the majority of the pores contributing to this conductance state. Alternatively, the presence of negatively-charged lipids in those membrane-invaginations lining the pore could be responsible for this phenomenon. In the future, more experiments with various ionic substrates will be performed for further clarification. Interestingly, currents elicited by supra-physiological voltages increased even after the 1–2 ms required for membrane charging and tended to level off only at the end of the 10 ms-pulse. This may reflect an increase in pore size in the millisecond range as predicted by theoretical modeling [44,45]. Since membrane conductance remained voltage-independent once a transition from the low- to the high-conductance state had occurred, the pores are probably formed almost instantaneously in one step but do not increase in size or number when the voltage is increased further.

In conclusion, this study paves the way for a more detailed patch clamp analysis of the electro-permeabilization of (plant) cell membranes. Experiments are under way to investigate the selectivity of the pores formed by supra-physiological voltages and the dependence of threshold potentials on various factors such as mechanical membrane tension, ion strength of the media, temperature, divalent cations, and pH.

Acknowledgments

Financial support for the shared research group "Physiological effect of pulsed electrical fields on plant cells" (SRG 60–1) partly funded by the "Karlsruhe Institute of Technology (KIT) Concept for the Future" within the framework of the German Excellence Initiative is gratefully acknowledged. LHW also acknowledges financial support by the German Ministry of Education and Science (BMBF; grant number 0315664B).

References

[1] J.M. Escoffre, T. Portet, L. Wasungu, J. Teissie, D. Dean, M.P. Rols, What is (still not) known of the mechanism by which electroporation mediates gene transfer and expression in cells and tissues, Mol. Biotech. 41 (2009) 286–295.
[2] M. Sack, C. Schultheiss, H. Bluhm, Triggered Marx generators for the industrial-scale electroporation of sugar beets, IEEE Trans. Ind. Appl. 41 (2005) 707–714.
[3] C. Gusbeth, W. Frey, H. Volkmann, T. Schwartz, H. Bluhm, Pulsed electric field treatment for bacteria reduction and its impact on hospital wastewater, Chemosphere 75 (2009) 228–233.

[4] A. Rieder, T. Schwartz, K. Schön-Hölz, S.M. Marten, J. Süß, C. Gusbeth, W. Kohnen, W. Swoboda, U. Obst, W. Frey, Molecular monitoring of inactivation efficiencies of bacteria during pulsed electric field (PEF) treatment of clinical wastewater, J. Appl. Microbiol. 105 (2008) 2035–2045.
[5] J. Teissie, M. Golzio, M.P. Rols, Mechanisms of cell membrane electropermeabilization: a minireview of our present (lack of?) knowledge, Biochim. Biophys. Acta 1724 (2005) 270–280.
[6] K.C. Smith, J.C. Weaver, Active mechanisms are needed to describe cell responses to submicrosecond, megavolt-per-meter pulses: cell models for ultrashort pulses, Biophys. J. 95 (2008) 1547–1563.
[7] U. Pliquett, R.P. Joshi, V. Srindhara, K.J. Schoenbach, High electrical field effects on cell membranes, Bioelectrochem. 70 (2009) 275–282.
[8] D.P. Tieleman, The molecular basis of electroporation, BMC Biochem. 19 (2004) 5–10.
[9] B. Flickinger, T. Berghöfer, P. Hohenberger, C. Eing, W. Frey, Transmembrane potential measurements on plant cells using the voltage-sensitive dye ANNINE-6, Protoplasma 247 (2010) 3–12.
[10] O.P. Hamill, A. Marty, E. Neher, B. Sakmann, F.J. Sigworth, Improved patch-clamp techniques for high-resolution current recording from cells and cell-free membrane patches, Pfluegers Arch. 391 (1981) 85–100.
[11] R.J. O'Neill, L. Tung, Cell-attached patch clamp study of the electropermeabilization of amphibian cardiac cells, Biophys. J. 59 (1991) 1028–1039.
[12] O. Tovar, L. Tung, Electroporation of cardiac cell membranes with monophasic or biphasic rectangular pulses, PACE 14 (1991) 1887–1892.
[13] O. Tovar, L. Tung, Electroporation and recovery of cardiac cell membrane with rectangular voltage pulses, Am. J. Physiol. 92 (1992) 1128–1136.
[14] A.G. Pakhomov, A. Bowman, B. Ibey, F. Andre, O. Pakhomova, K. Schoenbach, Lipid nanopores can form a stable, ion channel-like conduction pathway in cell membrane, Biochem. Biophys. Res. Com. 385 (2009) 181–186.
[15] A.G. Pakhomov, J.F. Kolb, J.A. White, R.P. Joshi, S. Xiao, K.J. Schoenbach, Long-lasting plasma membrane permeabilization in mammalian cells by nanosecond pulsed electric field (nsPEF), Bioelectromagnetics 28 (2007) 655–666.
[16] H.G.L. Coster, A quantitative analysis of the voltage–current relationships of fixed charge membranes and the associated property of the "punch-through", Biophys. J. 5 (1965) 669–686.
[17] M.J. Beilby, H.G.L. Coster, Effect of temperature on punchthrough in electrical characteristics of the plasmalemma of *Chara corallina*, Aust. J. Plant Physiol. 3 (1976) 819–826.
[18] T. Ohkawa, I. Tsutsui, Electrical tolerance (breakdown) of the *Chara corallina* plasmalemma: II inductive property of membrane and effects of pHo an impermeable monovalent cations on breakdown phenomena, J. Membr. Biol. 114 (1990) 159–173.
[19] H.G.L. Coster, U. Zimmermann, Dielectric breakdown in the membranes of *Valonia utricularis*. The role of energy dissipation, Biochim. Biophys. Acta 382 (1975) 410–418.
[20] H.G.L. Coster, U. Zimmermann, The mechanism of electrical breakdown in the membranes of *Valonia utricularis*, J. Membr. Biol. 22 (1975) 73–90.
[21] S.T. Meissner, Electroporation of the vacuole-attached patch clamp configuration allows access to the tonoplast resistance and estimation of its specific conductance, Plant Sci. 133 (1998) 91–103.
[22] T. Nagata, Y. Nemoto, S. Hasezava, Tobacco BY-2 cell line as the "Hela" cell in the cell biology of higher plants, Intern. Rev. Cytol. 132 (1992) 1–30.
[23] K.J. Führ, W. Warchol, M. Gratzl, Calculation and control of free divalent cations in solutions used for membrane fusion studies, Meth. Enzymol. 221 (1993) 149–157.
[24] E. Neher, Correction for liquid junction potentials in patch clamp experiments, Meth. Enzymol. 207 (1992) 123–130.
[25] B.A. Schmitt, H. Koepsell, An improved method for real-time monitoring of membrane capacitance in *Xenopus laevis* oocytes, Biophys. J. 82 (2002) 1345–1357.
[26] D.E. Goldman, Potential, impedance, and rectification in membranes, J. Gen. Physiol. 27 (1943) 37–60.
[27] B. Van Duijn, D.L. Ypey, K.R. Libbenga, Whole-cell K^+ currents across the plasma membrane of tobacco protoplasts from cell-suspension cultures, Plant Physiol. 101 (1993) 81–88.
[28] B. Van Duijn, Hodgkin–Huxley analysis of whole-cell outward rectifying currents in protoplast from suspension cultures, J. Membr. Biol. 132 (1993) 77–85.
[29] H. Stoeckel, K. Takeda, Plasmalemma voltage-activated K^+ currents in protoplasts from tobacco BY-2 cells: possible regulation by actin microfilaments? Protoplasma 220 (2002) 79–87.
[30] T. Sano, D. Becker, N. Ivashikina, L.H. Wegner, U. Zimmermann, M.R.G. Roelfsema, R. Nagata, R. Hedrich, Plant cells must pass a K^+ threshold to re-enter cell cycle, Plant J. 50 (2007) 401–413.
[31] T.Y. Tsong, Electroporation of cell membranes, Biophys. J. 60 (1981) 297–306.
[32] W. Chen, Supra-physiological membrane potential induced conformational changes in K^+ channel conducting system of skeletal muscle fibres, Bioelectrochem. 62 (2004) 47–56.
[33] W. Almers, Gating currents and charge movements in excitable membranes, Rev. Physiol. Biochem. Pharmacol. 82 (1978) 96–190.
[34] L.H. Wegner, A.H. De Boer, Activation kinetics of the K^+ outward rectifying conductance (KORC) in xylem parenchyma cells from barley roots, J. Membr. Biol. 170 (1999) 103–119.
[35] M. Heidecker, S. Mimietz, L.H. Wegner, U. Zimmermann, Structural peculiarities dominate the turgor pressure response of the marine alga *Valonia utricularis* upon osmotic challenges, J. Membr. Biol. 192 (2003) 123–139.
[36] M. Heidecker, L.H. Wegner, K.A. Binder, U. Zimmermann, Turgor pressure changes trigger characteristic changes in the electrical conductance of the tonoplast and the plasmalemma of the marine alga *Valonia utricularis*, Plant Cell Environm. 26 (2003) 1035–1051.
[37] T.F. McDonald, A. Cavalie, W. Trautwein, D. Pelzer, Voltage-dependent properties of macroscopic and elementary calcium channel currents in guinea pig ventricular myocytes, Pflügers Arch. 406 (1986) 437–448.
[38] A. Lebaudy, E. Hosy, T. Simonneau, H. Sentenac, J.B. Thibaud, I. Dreyer, Heteromeric K^+ channels in plants, Plant J. 54 (2008) 1076–1082.
[39] V.L. Soukhorukov, J.M. Endter, D. Zimmermann, R. Shirakashi, S. Fehrmann, M. Kiesel, R. Reuss, D. Becker, R. Hedrich, E. Bamberg, T. Roitsch, U. Zimmermann, Mechanisms of electrically mediated cytosolic Ca^{2+} transients in aequorin-transformed tobacco cells, Biophys. J. 93 (2007) 3324–3337.
[40] L.H. Wegner, A.H. De Boer, Properties of two outward-rectifying channels in root xylem parenchyma cells suggest a role in K^+ homeostasis and long-distance signalling, Plant Phys. 115 (1997) 1707–1719.
[41] F. Lemtiri-Clieh, E.A. MacRobbie, Role of calcium in the modulation of Vicia guard cell potassium channels by abscisic acid: a patch-clamp study, J. Membr. Biol. 137 (1994) 99–107.
[42] W. Chen, R.C. Lee, Altered ion channel conductance and ionic selectivity induced by large imposed membrane potential pulse, Biophys. J. 67 (1994) 603–612.
[43] W. Chen, Y. Han, Y. Chen, D. Astumian, Electric field-induced functional reductions in the K+ channel mainly resulted from supramembrane potential-mediated electroconformational changes, Biophys. J. 75 (1998) 196–206.
[44] R.W. Glaser, S.L. Leikin, V. Chernomordik, V.F. Pastushenko, A.I. Sokirko, Reversible electrical breakdown of lipid bilayers: formation and evolution of pores, Biochim. Biophys. Acta 940 (1988) 275–287.
[45] W. Krassowska, P.D. Filev, Modeling electroporation in a single cell, Biophys. J. 92 (2007) 404–417.
[46] S.W. Martin, B.J. Glover, J.M. Davies, Lipid microdomains—plant membranes get organized, Trends Plant Sci. 10 (2005) 263–265.